Nanoscale Advances

Accepted Manuscript

This article can be cited before page numbers have been issued, to do this please use: Md. S. Reza, Md. S. I. Tutul, T. Khandaker, C. Paul, Md. M. U. Haque and M. S. Hossain, *Nanoscale Adv.*, 2026, DOI: 10.1039/D6NA00060F.

ROYAL SOCIETY OF CHEMISTRY

rsc.li/nanoscale-advances

DOI: 10.1039/D6NA00060F

Eco-Friendly Starch-Nanocellulose Bio-Nanocomposite Films with Improved Structure-Property Interactions

Md. Shamim Reza[1], Md. Shahnawaj Islam Tutul[2], Tasmina Khandaker[3], Chironjit Paul[4], Md. Minhaz- Ul Haque[2], Muhammad Sarwar Hossain[4]*.

[1]Dept. of Civil Engineering, North Western University, Khulna-9100, Bangladesh.

[2]Dept. of Applied Chemistry and Chemical Engineering, Islamic University, Bangladesh

[3]Dept. of Chemistry, Pabna University of Science & Technology, Pabna-6600, Bangladesh.

[4]Chemistry Discipline, Khulna University, Khulna-9208, Bangladesh.

Abstract

The development of sustainable and biodegradable substitutes has increased due to the growing environmental concerns surrounding petroleum-based polymers. In order to assess the impact of nanocellulose fiber loading on the physicochemical, structural, thermal, optical, and mechanical properties of starch-nanocellulose bio-nanocomposite films, these films were created and thoroughly characterized. Using a straightforward solution-casting technique, sulfuric acid hydrolysis was used to remove nanocellulose from filter paper and incorporate it into a thermoplastic starch matrix plasticized with glycerol. Water uptake, moisture absorption, solubility, tensile testing, X-ray diffraction (XRD), thermogravimetric analysis (TGA), and UV-vis spectroscopy were used to make and evaluate composite films containing 0, 5, 10, and 20 weight percent nanocellulose. Because of reduced free volume and increased hydrogen bonding within the matrix, the results demonstrate that increasing the nanocellulose content dramatically decreased water uptake and moisture absorption. The use of nanocellulose enhanced film continuity and decreased cracking, as demonstrated by morphological observations. TGA showed increased thermal stability at larger nanocellulose loadings, while XRD examination showed a steady rise in crystallinity from 32% for clean starch to 60% for the 20-weight percent nanocellulose composite. Although elongation at break reduced as a result of higher stiffness, mechanical testing revealed significant increases in tensile strength and Young's modulus with increasing nanocellulose concentration. These results show that starch-nanocellulose composites have enhanced strength, thermal resistance, and barrier qualities, underscoring their great promise as environmentally benign materials for biodegradable packaging and associated uses.

Keywords: Starch, Nanocellulose, Bio-nanocomposites, Biodegradable films, Characterization

1. Introduction

In recent years, synthetic materials have been widely used in every stage of modern life such as shopping bags, furniture etc. [1, 2]. Synthetic materials are more durable, versatile, uniform and environmentally sustainable, but most of the synthetic materials are expensive and need high processing cost. Besides these synthetic materials are inert to microorganism attack, cause disposal problem, and create serious environmental pollution. At present macromolecular substances are produced from petroleum. Most petroleum-derived polymers are not biodegradable and persist in the environment [3, 4]. But some are not biodegradable. Considering these issues, natural polymeric composite need to be developed and make them sustainable, suitable to use, easy disposal and make them sustainable, suitable to use, easy disposal and make them alternative source to synthetic materials. For this, among different natural polymers, starch is of great interest. It is a linear polymer. It is easily obtained from plant sources such as potato, corn wheat, maize etc. It is a semi-crystalline polymer. It has two units as amylose and amylopectin. Amylose is a linear polymer chain and amylopectin is a branching structure. Both of these units are attached with glycoside bond. Due to presence of more hydroxyl groups, it shows hydrophilic nature and forms hydrogen bond with ether and alcohol. It is not a thermoplastic like synthetic materials in cold water, but in hot water, it breaks down glycoside bond and turns into thermoplastic nature [5, 6].

Starch is considered a promising source for bio-composites owing to its biodegradability, renewability, and environmentally friendly nature [7, 8]. Bio-composites are formed by combining heterogeneous materials to achieve properties superior to those of the individual components. Despite these advantages, starch-based polymeric materials exhibit inherent limitations, such as high moisture sensitivity and relatively low mechanical strength. These drawbacks can be effectively addressed by incorporating cellulose fibers as reinforcing fillers and glycerol as a plasticizer, which enhance stiffness, interfacial bonding, and overall durability [9, 10]. Furthermore, compared to conventional natural cellulosic fiber-based systems, nanocellulose-based composites have emerged as advanced materials, offering remarkable improvements in mechanical performance at low Fiber loadings while preserving transparency, processability, and sustainable characteristics [11, 12]. Extracted from a variety of natural sources, nanocellulose has been utilized extensively to increase mechanical strength and decrease water sensitivity. In order to extract them, non-cellulosic components are usually removed by chemical or biological pretreatments [13-15].

View Article Online
DOI: 10.1039/D6NA00060F

Starch-nanocellulose composites have gained significant attention as sustainable bio-composite materials due to the reinforcing potential of cellulose nanofibers (CNF). CNF act as effective nano-scale fillers within starch matrices, leading to notable improvements in mechanical strength, thermal stability, and controlled degradation behavior. Owing to the hydrophilic nature of cellulose systems, increased surface roughness and strong interfacial interactions between starch and nanocellulose play a crucial role in enhancing composite performance [16-18]. Various surface modification and processing strategies for nanocellulose have been explored to further tailor the structural and functional properties of these composites [19-21]. As a result of their small dimensions, high surface reactivity, and organized assembly, starch-nanocellulose composites exhibit superior stiffness and strength at low filler loadings. These advantageous characteristics make them highly suitable for a wide range of applications, including packaging, construction, automotive components, furniture, electronics, as well as emerging uses in pharmaceutical, cosmetic, and biomedical fields [22, 23].

Glycerol is added to increase composite's flexibility, water resistivity, and sustainability. It increases water resistivity and sustainability of bio-composite film. Earlier, thermoplastic starch is mixed with polyethylene glycol, polycaprolactone, polybutylene, and polyhydrobutyrate as plasticizer for bio-composites. But the blends of thermoplastic starch with polycaprolactone, polybutylene, polyethylene, glycol shows brittleness as well as immiscible and lower flexibility. Overcoming this problem, glycerol is added with thermoplastic starch, which reduces brittleness and increase flexibility and procesability of composite films [24, 25]. The combined development and methodical assessment of totally biodegradable starch-nanocellulose bio-composite films employing a straightforward solution-casting fabrication technique and a techno-economically feasible chemo-mechanical extraction process for nanocellulose constitute the novelty of this study. This work offers a thorough correlation between physicochemical, thermal, structural, optical, and mechanical properties through combined solubility, moisture and water absorption, film integrity, thermo gravimetric analysis (TGA), x-ray diffraction (XRD), UV-vis spectroscopy, and tensile analyses, in contrast to many earlier studies that concentrate on limited property assessment. In order to achieve balanced mechanical strength, thermal stability, and biodegradability, the study specifically focuses on optimizing nanocellulose reinforcement within a thermoplastic starch matrix plasticized with glycerol. This work advances starch-based nanocomposites toward feasible, scalable, and commercially relevant biodegradable material alternatives by simultaneously addressing process simplicity, sustainability, and performance.

View Article Online
DOI: 10.1039/D6NA00060F

2. Materials and Methods

2.1 Materials

Starch and Cellulosic fiber were the raw materials for the preparation of polymeric composite. Where Strach was collected from the local market as well as nanocellulose was extracted from filter paper. Sulfuric acid (H_2SO_4) purity 98% manufacturer BDH (England), Glacial acetic acid (CH_3COOH) purity 100% manufacturer BDH (England), Methanol & Ethanol (C_2H_5-OH) manufacturer BDH (England), Di-methyl sulfo-oxide manufacturer E. Marck Ltd. Germany, Glycerol was collected from Dhaka, Bangladesh.

2.2 Methods

2.2.1 Preparation of Nanocellulose from Filter Paper

Cellulose nano-fibres were prepared by the twice-acid hydrolysis of filter paper. The hydrolysis was carried out with H_2SO_4 solution (60 wt. %) at 45°C under continuous stirring. The fibre to liquor ratio was 1:10 (10 ml of sulphuric acid for 1 g of cellulose). After 50 minutes, the hydrolysis was stopped by adding 5-fold excess distilled water (50 ml) to the reaction mixture. The resulting mixture was cooled down to room temperature and centrifuged. The solid fraction was washed off by distilled water until to obtain a neutral pH. The hydrolysis was carried out again following the above procedure. Finally, the nanocellulose suspension was obtained by stirring the solid fraction with required amount of water. The newly generated suspension was stored in refrigerator at 4°C.

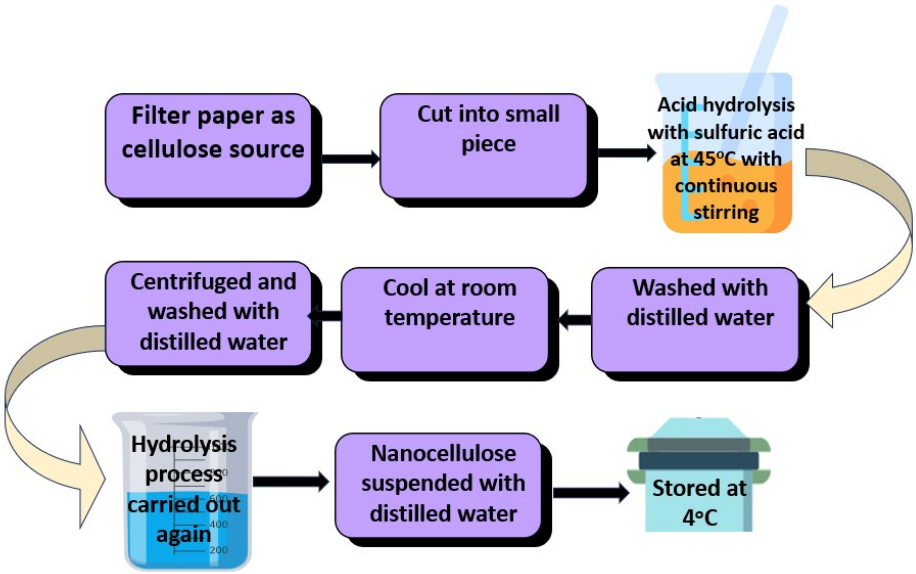

Figure 1. Block diagram of nanocellulose preparation.

View Article Online
DOI: 10.1039/D6NA00060F

2.2.2 Starch Film Preparation

4 gm starch, 1 gm glycerol, 0.21 gm acetic acid were taken in a beaker and heated with constant stirring. When the mixture was concentrated poured the mixture on a Petridis. After keeping 24 hours in an open air, the mixture was turned into film. Then the films were heated at 60°C. This film was continuous and flexible. Finally, the dried film was collected and stored.

2.2.3 Composite Films Preparation

Though there were minor differences in the formulation during the initial stage of preparation, the impact on the final properties has been regarded as negligible compared to the reinforcing effect of the nanocellulose. This have been made to reflect the compositions and results based on such a consideration.

2.2.3.1 Composite containing 5 wt. % nano-cellulose fibers

3.5 gm of starch, 1.5 gm of glycerol, 0.18 gm of acetic acid and 0.25 gm of nanocellulose (5 wt. % nanocellulose) with 50 ml of distilled water were taken in a beaker and heated with constant stirring. When the mixture was turned into concentrated, then the mixture was poured on a petridis to make film, kept the films for 24 hours in an open air, and heated at 60°C. Finally, the dried films were collected and stored.

2.2.3.2 Composite containing 10% nanocellulose

3.5 gm of starch and 50 ml of distilled water were mixed well. Then, 1.5 gm of glycerol; 0.18 gm acetic acid and 0.5gm nanocellulose (10 wt % nanocellulose) were mixed with the previous mixture, heated, and stirred until the mixture was concentrated. When the mixture was turned into concentrated, poured the mixture on a Petridis and kept it for 24 hours. After 24 hours, the mixture was turned into continuous composite film. Then the film was heated at 60°C and dried film was collected and stored.

2.2.3.3 Composite containing 20% nanocellulose fiber

3.5 g of starch, 1.5 g of glycerol, 0.18 g of acetic acid, 50 ml distilled water were mixed well. Then 1 g nanocellulose fiber was mixed with the previous mixture and heated with stirring until the mixture was turned into concentrated, poured the mixture on a petridis and kept it for 24 hours in an open air. When the mixture as turned into composite film, dried at 60°C and collected the dried composite film.

View Article Online
DOI: 10.1039/D6NA00060F

3. Analytical Method and Analysis

A digital screw was used to measure the films thickness. The films thickness was measured which was 0.25 mm. The film was dried at 60°C for 4 hours to get constant weight and kept the film in a desiccator. The dried films were examined by naked eye and the film was analyzed with various parameter. For exact measurement, at least five measurements for each film were done.

3.1 Water Absorption Behavior of Starch-Nanocellulose Composite Films

The composite film was dried at 60°C for 4 hours to get constant weight and kept the film in a desicator. The-dried film samples were sectioned into pieces of uniform size (e.g., 20 mm x 20 mm) and average thickness ~0.10 mm. Those small pieces of composite films were kept under different solvents in several test tubes. After three hours, the films were taken out of 50 mL water and excess water was removed by using tissue paper. After this, the films were weighed. From the increased amount of weight and the initial weight, the water absorption capacity was observed.

3.2 Moisture Absorption Test

At first, the films were dried at 60°C to keep constant weight. Film samples of identical dimensions were weighed and noted down the result. Now a beaker with 50 mLwater was taken and metal wire net was kept on the beaker and films were kept upon the wire mesh. The dried films were kept on the wire mesh and kept for 24 hours and weighed. From the previous weight and the final weight, the percent of moisture absorption was calculated. The formula for moisture absorption percentage was as

$$\%\ moisture\ adsorbance = \frac{Final\ weight - Original\ weight}{Original\ weight} \times 10$$

3.3 Solubility Test

The solubility of the prepared composite films was assessed by using a qualitative method. For the experiment, film samples were cut to uniform sizes (about 20 mm × 20 mm) with a uniform thickness of ~0.10 mm and placed in different test tubes containing 50 mL of different solvents such as methanol, ethanol, chloroform, distilled water, dimethyl sulfoxide (DMSO), and acetone. The samples were kept in different conditions such as room temperature and high-temperature conditions using a water bath (60 ± 2 °C) for 3 hours. After the desired time, the samples were checked visually for signs of dissolution and disintegration.

View Article Online
DOI: 10.1039/D6NA00060F

3.4 Thermo-gravimetric analysis

Thermo-gravimetric analysis of starch-based bio-nanocomposite film was conducted using a TGA/DTA made by Parker Elmer, measured the weight loss of a sample as a function of temperature. This was done by placing a sample into a sample holder that hangs from a micro-gram balance during the entire experiment. The balance mechanism consisted of a sample pan holder suspended by a long hang down wire. The hang down wire was connected with the balance lever by a small quartz link to prevent static build up. The weight of the sample holder configuration was electrically balanced on the other side so that the balance could be zero before each run. TGA was run from room temperature to 600 degrees centigrade at a rate of 10 degree centigrade per minute under nitrogen atmosphere. For high accuracy, every analysis was done two times for each sample.

3.5 Tensile test

Tensile tests were performed using an Instron 8821S tension meter. The tensile specimens were cut in rectangular shapes with dimensions of 65 mm in length and 10 mm in width. The gauge length was fixed at 50 mm and the cross head speed was 5 mm/min at room temperature. A basic mechanical assessment technique called tensile testing is used to find out how a material reacts to a tensile force. It is one of the easiest and most used tests for evaluating mechanical performance. Designers and quality managers can forecast how materials and products will behave under actual service circumstances by determining the force needed to stretch a specimen till failure. The findings guarantee that the materials, parts, and final goods are suitable for their intended uses by offering vital information on their integrity, dependability, and safety.

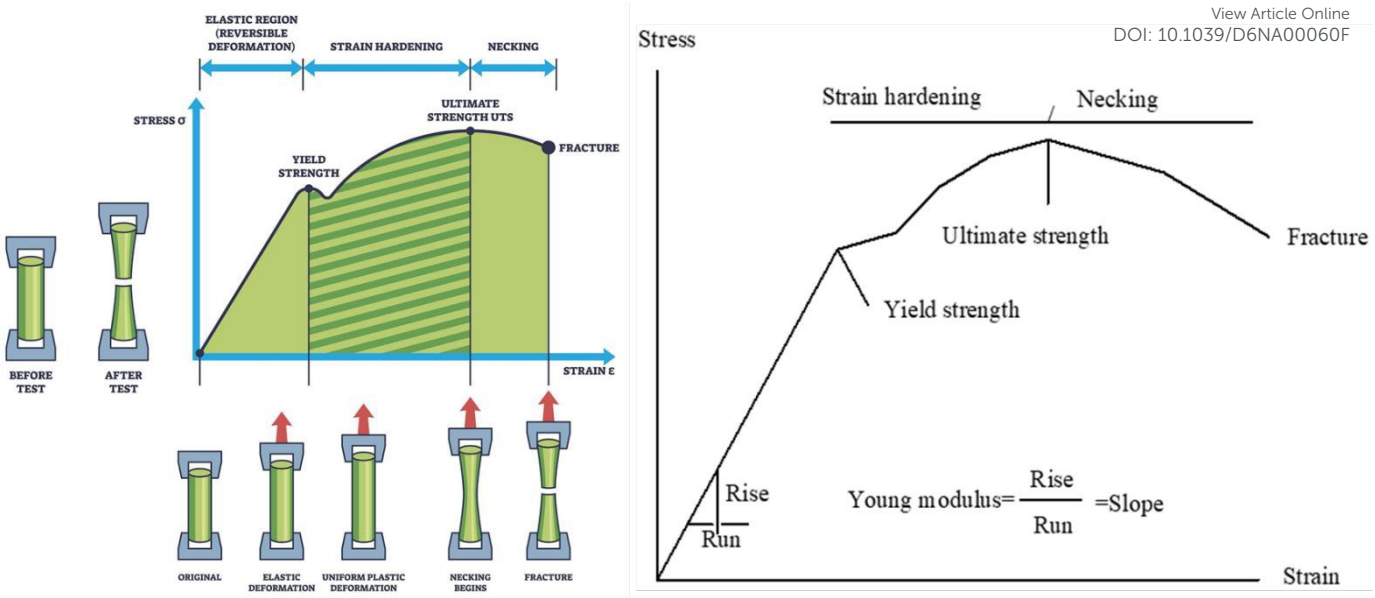

Figure 2. Illustration of elastic deformation, yield strength, strain hardening, ultimate tensile strength, necking, and various types of fracture by representative stress-strain curves, and how they would compare to actual specimen shape problems during tensile testing [26].

The stress-strain curve is a graphical representation of the relationship between the stress applied to a material and the amount of elongation that occurs due to that stress when subjected to a tensile load as shown in fig. 2. The elastic portion will be a straight line, indicating that the material is in the elastic region before it reaches its yield strength and plastic deformation begins. After yielding, the material will continue in plastic deformation (strain hardening) until it reaches its ultimate tensile strength. After reaching its ultimate tensile strength, the material will undergo necking (reduction of cross-section) which ultimately leads to failure (fracture) of the material.

Stress is a measure of the internal force per unit cross sectional area. The formula for calculating stress is the same as the formula for calculating pressure as

$$\sigma = {}^{F}/_{A} \dots\dots\dots\dots\dots\dots\dots (1)$$

Where, σ is the stress, F is the applied force per unit area, A is the cross sectional area of the sample.

Stresses cause strain. Applying pressure on an object causes it to stretch. Strain is a measure of how much an object is being stretched. The formula for strain is:

$$\in = \frac{L - L_0}{L_0} \dots\dots\dots\dots\dots\dots\dots\dots\dots (2)$$

View Article Online
DOI: 10.1039/D6NA00060F

Where L_o is the original length of a bar being stretched, and l is its length after it has been stretched. (L-L_o) is the extension of the bar, the difference between these two lengths

The (ultimate) tensile strength is the level of stress at which a material (rope, wire, or a structural beam) will fracture. Tensile strength is also known as fracture stress. The breaking load of a material was measured in Newton (N).Stress and strain was calculated using the following formula given below as,

$$Tensile\ stress = \frac{Breaking\ Load\ (N)}{Thickness\ \times\ Width} = {}^{N}/_{mm^2} \ldots\ldots\ldots\ldots\ldots\ldots\ldots\ldots (3)$$

$$Tensile\ strain = \frac{Elongation}{Initial\ length} \times 100 \ldots\ldots\ldots\ldots\ldots\ldots\ldots\ldots (4)$$

Young's Modulus is a measure of the stiffness of a material. It states how much a material will stretch as a result of a given amount of stress. The formula for calculating it is:

$$E = {}^{\sigma}/_{\epsilon} \ldots\ldots\ldots\ldots\ldots\ldots\ldots\ldots\ldots (5)$$

Where, σ is tensile stress and € is tensile strength.

The elongation of the specimen expressed as a percentage of the gage length.

$$\%\ of\ Elongation = \frac{Final\ Length - Original\ length}{Original\ length} \times 100$$

3.6 UV spectroscopy

Ultra violet spectroscopy refers to absorption spectroscopy or reflectance spectroscopy in the ultra violet region. The absorption or reflectance in the visible range directly affects the perceived color of the chemicals involved. In this region of the electromagnetic spectrum, molecules undergo electronic transition. This technique is complementary to florescence, in that florescence deals with transitions from the the excited state to the ground state, while absorption measures transitions from the ground state to the excited state. Samples were cut into 0.25mm wide and 3cm log and placed the samples into sample holder and took the result and noted down the results.

3.7 X-Ray Scattering

X-ray defection analysis of pure polymers, fibres, blends and composites was performed at room temperature with a Siemens Kristalloflex 810 diffractometer operating at 40 kV and 30 mA, using the CuKa radiation (λ= 0.1546 nm). The crystalline degree of the samples was

View Article Online
DOI: 10.1039/D6NA00060F

determined as the ratio of the areas of crystalline reflections to the whole area (after subtraction of background) in the 2θ range.

4. Results and Discussion

4.1 Morphology Analysis

Figure 3 (a-d) shows what the films look like when we add nanocellulose to them. The film that is starch (a) is not very clear and it breaks easily. It also does not look the same over. When we add a little bit of nanocellulose to the starch like 5-20 percent (b-d) the film gets smoother and it is easier to bend. This means that the tiny particles in the film are working together better and the film is stronger. We took these pictures with a camera, not a special microscope. Optical clarity, surface homogeneity, and mechanical reinforcement are all affected by the gradual addition of nanocellulose fibers, underscoring the significance of fiber concentration in adjusting the physicochemical characteristics of starch-based bio-nanocomposite films for possible biodegradable packaging applications [27].

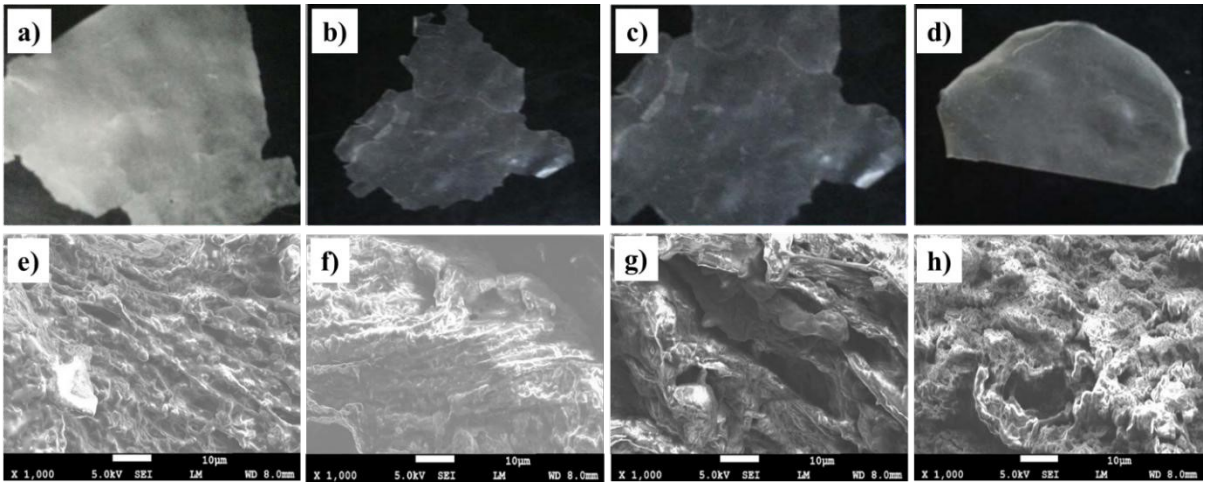

Figure 3. Photographic images of (a) neat starch film and starch–nanocellulose composite films containing (b) 5 wt%, (c) 10 wt%, and (d) 20 wt% nanocellulose fibers; SEM micrographs of (e) neat starch film and composites with (f) 5 wt%, (g) 10 wt%, and (h) 20 wt% nanocellulose fibers.

So Figure 3 helps us see how clear and uniform the films are. It does not show us what the surface of the film looks like in detail. The pictures at the bottom (e-h) are from a microscope that helps us see the tiny details on the surface of the film like how rough it is and how the fibers are spread out. These special microscope pictures show us that when we add nanocellulose to the starch the film gets more compact and the particles are connected better. There are also empty spaces in the film. This is important because it helps the film be stronger

View Article Online
DOI: 10.1039/D6NA00060F

and work better. We need to look at the film with this microscope because it shows us things that we cannot see with other tools. In order to confirm the successful extraction of nanocellulose, a detailed characterization of the morphological properties of nanocellulose was examined. From the SEM images (Figure 3e-h), it can be seen that there are fibrillar structures and interconnected structures. This shows that nanoscale cellulose fibers have been formed. The decrease in fiber size and improved distribution within the composite matrix show that acid hydrolysis and defibrillation were successful. Although the size of individual nanofibers cannot be precisely determined based on the resolution limit, the morphology shows good agreement with those reported for nanocellulose. So when we look at the pictures (Figure 3a-d) and the special microscope pictures (Figure 3e-h) together we can understand how the structure of the film affects its properties. This is important, for starch. nanocellulose bio-nanocomposite films.

4.2 Water Uptake Analysis

Water uptake test was done with the different types of dried composite films in figure 4. The water uptake capacity of starch and its composites film by the addition of nano-cellulosic fibers. From this figure it is clear that the water uptake capacity was highest for the pure starch film and lowest water absorption capacity was for the composite film which contain 20 wt % nano-cellulose. This is well known that glycerol containing hydroxyl groups and starch is highly hygroscopic in nature. For this reason, the highest water absorption was occurred in starch composite without nano- cellulosic fibers. On the other hand, the diminution of water content was occurred and free volume among starch molecules were reduced due to the addition of nano-cellulosic fibers in the composite films. That is why, water absorption was reduced to the lowest point for the composite containing 20 wt % nanocellulosic fibers showed in figure 4.

4.3 Moisture Absorption Analysis

Starch is highly hygroscopic material and produced from natural sources. From the figure 4, it was seen that the addition of nanocellulose content on the starch-based composite reduced the moisture absorption capacity of the starch film and its composites. Because, addition of nanocellulose reduced the free volumes of starch. From some previous work on starch-based composites, it was noted that a slight diminution of water content was observed with the addition of nanocellulose content [19-20]. Besides this, glycerol contains hydroxyl groups. As a result, due to addition of glycerol content in composite formulation, glycerol increased

View Article Online
DOI: 10.1039/D6NA00060F

moisture absorption capacity. Highest moisture absorption capacity was observed for the composite without nanocellulosic fiber (1.15%) and lowest moisture absorption capacity was for the composite containing 20 wt % nano-cellulose content (0.88% to 0.81% decrease) shown in figure 4.

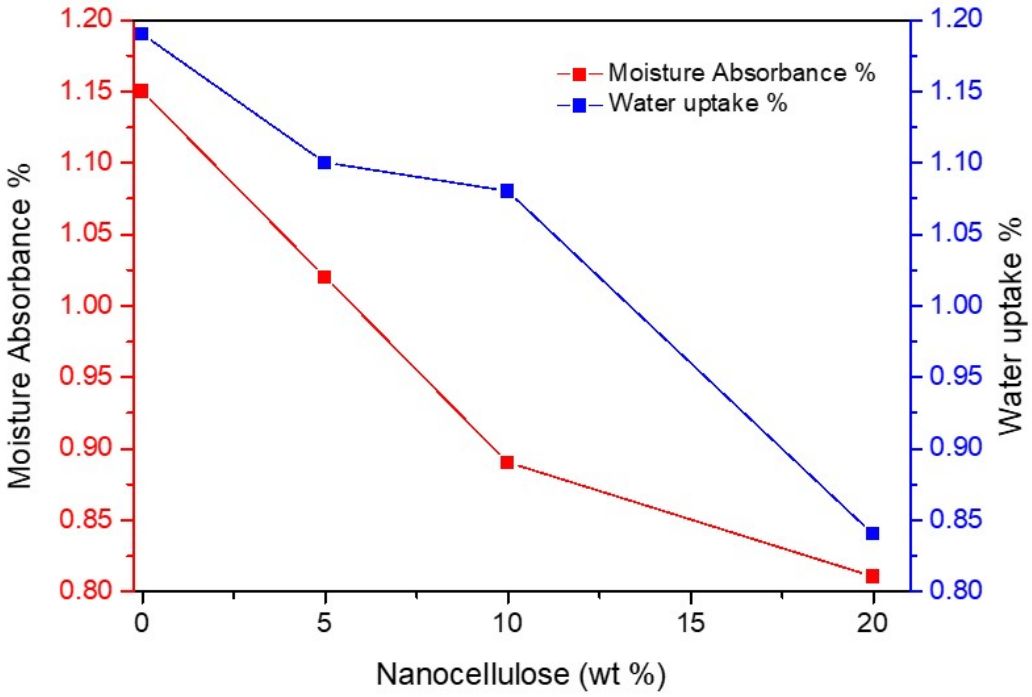

Figure 4: Moisture absorption and water uptake test with nanocellulose percentage.

4.4 Nanocellulose's Function in Preventing Starch-Based Film Cracking

From the observation of films, it was noted that film of 100 wt % starch was cracked and not continuous due to break down of glycoside bond of starch showed in figure 4. It is also found that Micro-organism can be grown on film if it be on dark and cool place during processing period. On the other hand, Continuous and un-cracked films were obtained when 5 wt %, 10 wt %, & 20 wt % of nano-cellulose were added to the composite. This was due to nanocellulose binds starch and reduces free volume of starch [28].

4.5 Solubility Test

A small piece of starch-based nano-cellulosic composite film was immersed in different solvents taken in a test tube in both normal (25°C) and hot (60°C) condition. To observe the solubility of sample namely distilled water, acetone, chloroform, methanol, ethanol, dimethyl sulphoxide were selected as solvents. And finally, it was found that the starch-based nano-cellulosic composite films were dissolved in dimethyl sulphoxide.

View Article Online
DOI: 10.1039/D6NA00060F

4.6 X-ray diffraction (XRD) Analysis

The structure of starch and starch with nanocellulose films was looked at using X-ray diffraction. The patterns showed peaks that're typical of starch and also had contributions from nanocellulose. When nanocellulose was added it changed the intensity and sharpness of the peaks, which means the structure of the composite was changed. The crystallinity index was calculated using a method called the Segal method. This method uses the intensity of the crystalline peak and the lowest intensity of the amorphous region. The formula is:

$$Crystallinity\ index = [{}^{(I_{002} - I_{am})}/_{I_{002}}] \times 100$$

Here, I_{002} is maximum intensity of the crystalline phase and I_{am} is amorphous scattering. This method gives an idea of how crystalline the composite is. The X-ray diffraction patterns come from both starch and nanocellulose. So the crystallinity values are for the composite, not just the individual parts. This means that the changes in crystallinity should be seen as changes, in how the structures ordered because nanocellulose was added, rather than a direct comparison of how crystalline each part is. Table 1 summarizes the relevant crystallinity values. A large diffraction halo in the 2θ range of roughly 15-23° is seen in neat starch. This is typical of gelatinized or processed starch, where natural crystalline domains are destroyed during film production, and is indicative of a primarily amorphous or semi-crystalline structure [29]. As a result, plain starch exhibits a comparatively low crystallinity of 32%. Table 1 displays the crystallinity percentages, which increase as the volume percentage of nanocellulose increases. Moreover, the increase in crystallinity as determined from XRD results shows that highly crystalline cellulose structures have formed, as observed for nanocellulose.

Table 1: Calculated crystallinity of starch and its composites with nano-cellulose by XRD analysis

Sample	Compositions	Crystallinity, %
Starch	100/0	32
Starch/NC 95/5	95/5	52
Starch/NC 90/10	90/10	53
Starch/NC 80/20	80/20	60

The diffraction profiles clearly and systematically alter when nanocellulose is included. Increased peak intensity and more distinct diffraction characteristics are seen in the starch/NC

composites, especially around 2θ = 16–17° and 22–23°, which correlate to the distinctive reflections of cellulose I crystalline planes. A substantial sharpening of peaks is visible with a modest NC loading of 5% (Starch/NC 95/5), suggesting a minor improvement in molecular ordering and an increase in crystallinity to 52%. The diffraction peaks get sharper and more intense as the NC component is increased to 10% and 20%, indicating improved structural organization. The Starch/NC (80/20) composite has the maximum crystallinity of 60%. The naturally high crystalline nature of nanocellulose and its efficient function as a nucleating and reinforcing agent within the starch matrix are responsible for the progressive improvement in crystallinity with increasing NC concentration. Better chain packing and the creation of more ordered domains are encouraged by strong intermolecular hydrogen bonds between the hydroxyl groups of starch and nanocellulose. So, the XRD data show that adding nanocellulose greatly enhances the crystalline structure of starch-based composites, which is anticipated to have a favorable impact on their mechanical strength and barrier qualities.

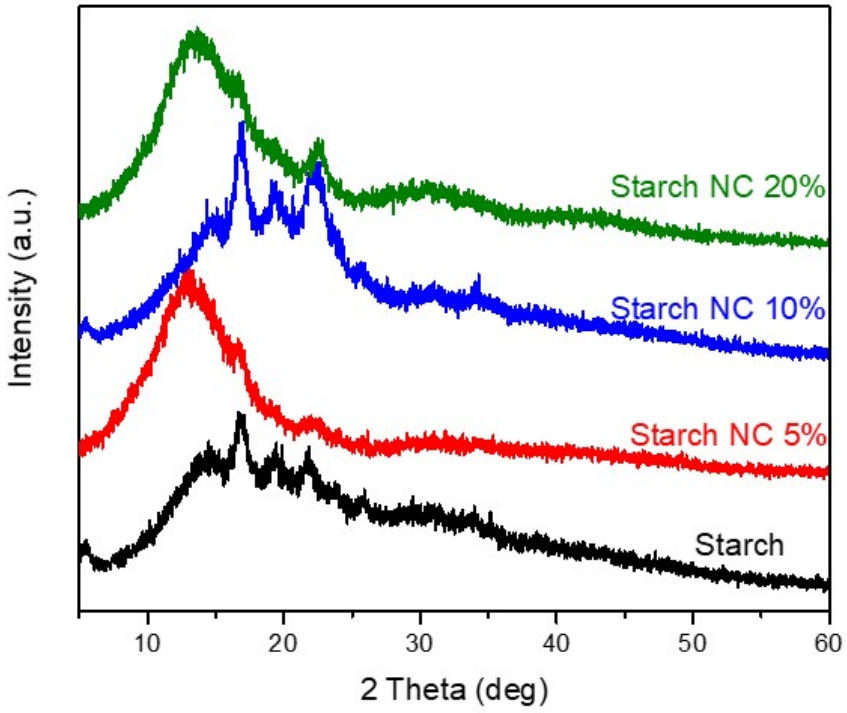

Figure 5. X-ray diffraction data for Starch-nanocellulose composites

4.7 Optical properties

The optical properties of starch and starch-nanocellulose films were looked at using a special tool called UV-vis spectroscopy. The results are shown in Figure 6. When we look at the absorbance spectra in Figure 6a we see that the absorbance goes up as the nanocellulose content

View Article Online
DOI: 10.1039/D6NA00060F

increases. This means that the light is being scattered more inside the matrix. On the hand the transmittance spectra in Figure 6b show that the light transmission goes down a lot as the nanocellulose loading increases from 0 to 20 wt.%. To be specific the transmittance goes down from about 63% for starch to 42%, 19% and 10% for films that have 5, 10 and 20 wt.% nanocellulose. This decrease in transparency is because the crystallinity increases and ordered structures are formed, which makes it harder for light to pass through the films. Also the increase in absorbance when nanocellulose is added suggests that the internal microstructure of the films is changing and that the nanocellulose might be aggregating or not dispersing evenly at loadings. Even though the transmittance is reduced all the films are still somewhat transparent which we can see with our eyes. There are no clumps visible which is good. These results show that the amount of nanocellulose in the films is very important, for how they behave with light and how they are structured. The starch-nanocellulose composite films and their optical properties are really affected by the nanocellulose content and the way the nanocellolose is organized inside the films.

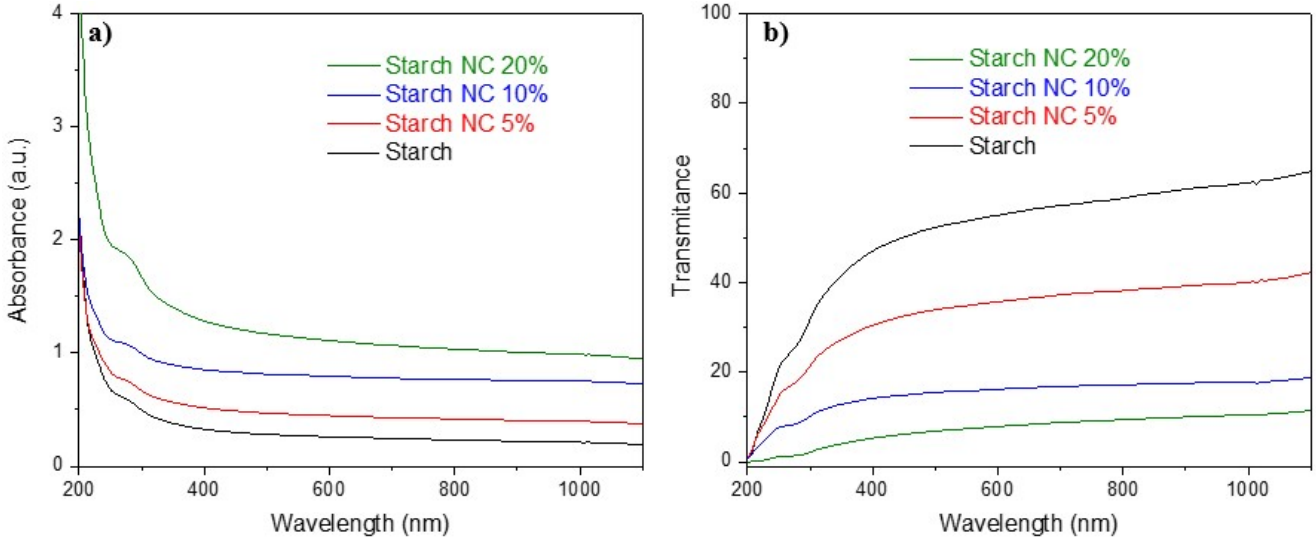

Figure 6. UV-vis absorbance and transmittance spectra of Nanocellulose-starch composites in different ratios.

4.8 Thermal analysis

This analysis is carried out to measure the thermal stability of starch based bionano composite. TGA, DTG curve are shown in figure 7.

The thermal stability and degradation behavior of clean starch and starch–nanocellulose composite films were assessed using TGA; the associated TG and DTG curves are displayed in Figures (a) and (b), respectively. The TG curve for plain starch indicates a first weight loss

View Article Online
DOI: 10.1039/D6NA00060F

that starts at about 31.9 °C. The elimination of physically absorbed moisture is responsible for roughly 10.1% of the mass loss. The breakage of starch molecular bonds causes the primary degradation process, which has onset temperatures of 149.3, 306.3, and 346.5 °C. This results in a total mass loss of roughly 67.9%. A tiny leftover mass remains after the degrading process is finished at 346.5 °C. The initial weight loss for starch-based films with plasticizer but no nanocellulose begins at about 29.4 °C, and the removal of moisture causes a 6.9% mass loss at about 111.4 °C. With an overall degradation of 54.8%, the primary degradation stage exhibits onset and maximum breakdown rates at 281.4, 315.6, and 348.9 °C. Up to 490 °C, there is an additional weight loss of roughly 21.9%, which is mostly related to ongoing volatilization and disintegration. The first moisture-related weight loss in the starch/NC composite films is around 10.2%. This is followed by a severe degradation stage when the breakdown of amylose and amylopectin chains causes about 65.3% mass loss. At 248.3, 296.9, and 351 °C, the corresponding onset and maximum degradation temperatures are noted.

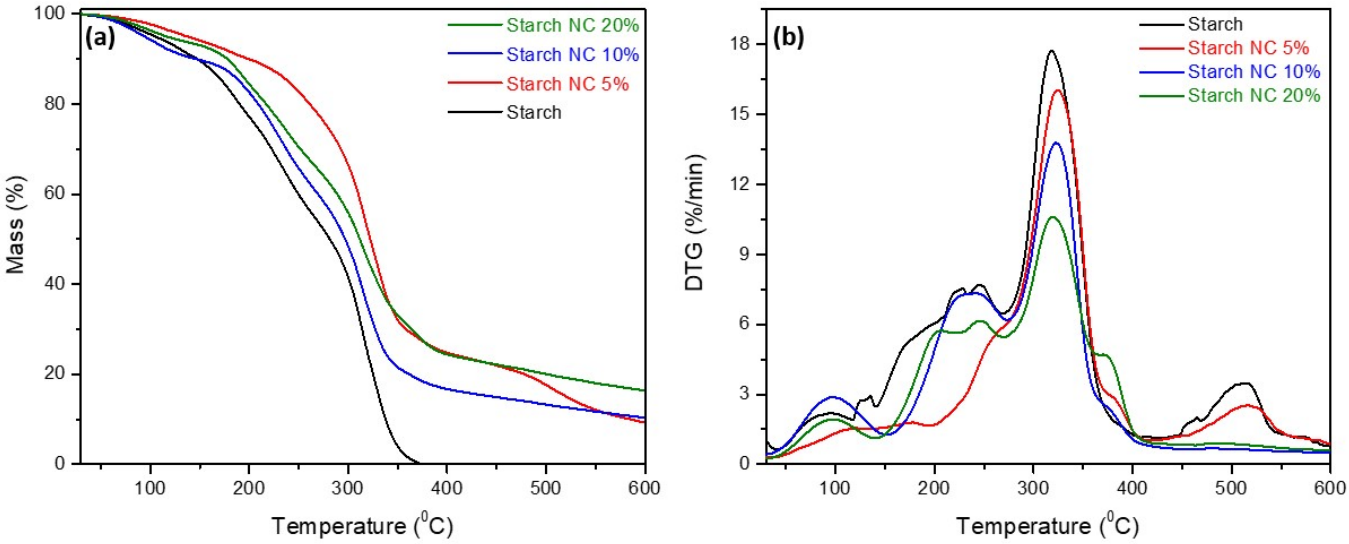

Figure 7. TGA curves (a) and DTG curves (b) for Starch-nanocellulose composites containing different ratios.

Another composite exhibits an initial moisture loss of 6.4%, with significant deterioration (56.2%) taking place at maximum slopes and onset temperatures of 239, 300.2, and 364 °C, and degradation finishing at about 364 °C. Moisture and volatile removal account for an additional 18.1% of the mass loss; the ash content of the composite film is responsible for the remaining residue. In contrast, composites with 20% nanocellulose show a wider and shifted degradation range from about 239.1 to 364.1 °C, indicating improved thermal stability, while composites without nanocellulose show degradation onset at about 267 °C and completion at

View Article Online
DOI: 10.1039/D5NA00060F

about 346.5 °C. Glycerol and starch break down at about 240 °C and 290 °C, respectively, whereas cellulose requires more energy to break down because of its strong glycosidic linkages and stiff glucose chains; it usually breaks down between 300 and 395 °C. The addition of nanocellulose improves the composites' overall thermal resistance; the film with 20% nanocellulose showed the highest breakdown temperature. This behavior is explained by the build-up of glycerol at the amylopectin-nanocellulose interface, which encourages the development of crystalline areas surrounding nanocellulose fibers. The inorganic and carbonaceous components of the starch-based composite films are represented by the stable solid residue that is left over after heating over 440 °C.

4.9 Mechanical properties

The mechanical property of starch-nanocellulose bio-nanocomposite films was determined using the stress-strain curve (Figure 8), and the obtained data is listed in Table 2 in the form of Mean ± Standard Deviation, which ensures the reliability of the obtained data with the calculated values using the corrected cross-sectional area and gauge length.

Table 2. Tensile strength, Young's modulus, and elongation at break of starch–nanocellulose bio-nanocomposite films with different NCF loadings

Materials	Tensile strength (MPa)	Young modulus (MPa)	Elongation at break (%)
0% NCF	2.7±0.15	100.0±6.0	2.4±0.17
5% NCF	3.2±0.10	143.0±9.0	2.0±0.10
10%NCF	4.0±0.19	192.1±15.2	2.2±0.11
20% NCF	4.5±0.26	250.5±13.6	1.6±0.10

From the calculation, it is found that there is a clear correlation between Figure 8 and Table 2. The neat starch film (0 % NCF) shows the lowest tensile strength (2.7 ± 0.15 MPa), Young's modulus (100.0 ± 6.0 MPa), but the highest elongation at break (2.4 ± 0.17%) compared with the starch-nanocellulose bio-nanocomposite films. The starch-nanocellulose films show improved tensile strength and modulus with the addition of nanocellulose fibers. As the NCF loading increases to 5% NCF, the tensile strength increases to 3.2 ± 0.10 MPa, and Young's modulus increases to 143.0 ± 9.0 MPa. The elongation decreases slightly to 2.0 ± 0.10%. This indicates the efficient stress transfer due to the enhancement of the interfacial interaction and the dispersion of the nanocellulose.

View Article Online
DOI: 10.1039/D6NA00060F

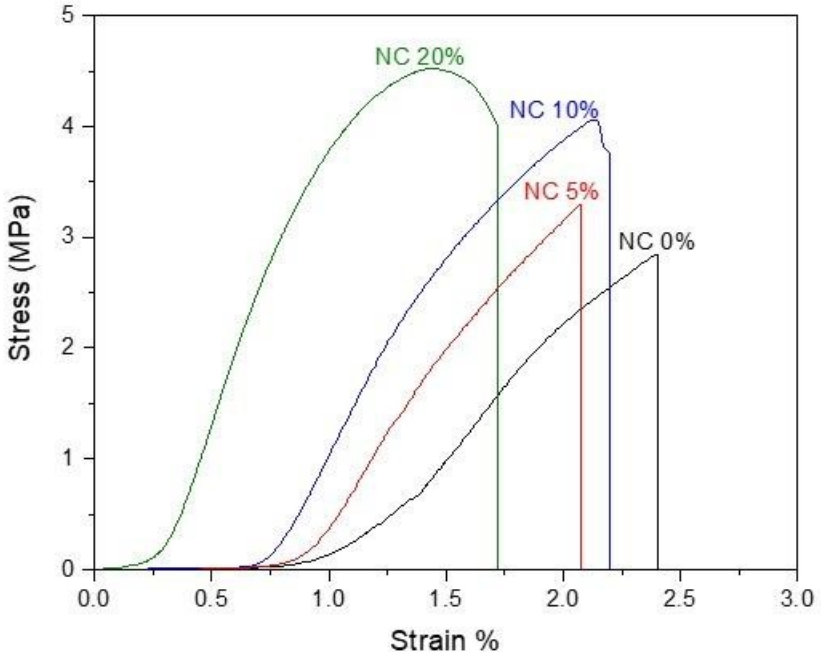

Figure 8: Stress vs Strain curve for Starch-nanocellulose composites containing different ratios.

When the NCF content in the composite increases to 10%, the tensile strength and Young's modulus increase to 4.0 ± 0.19 MPa and 192.1 ± 15.2 MPa, respectively. The elongation decreases slightly to 2.2 ± 0.11%. The trend observed in Figure 8 and Table 2 indicates the enhancement of the composite without abnormal deviation. The maximum mechanical property is obtained for 20% NCF composite, where the tensile strength is 4.5 ± 0.26 MPa, and Young's modulus is 250.5 ± 13.6 MPa. The ductility of the composite is reduced to 1.6 ± 0.10% with an increase in nanocellulose content. Finally, it is evident from the corrected results that there is an increasing trend for tensile strength and stiffness with an increase in nanocellulose content, whereas ductility is reduced. The results obtained from recalculating the data (Table 2) and stress-strain curves (Figure 8) show an agreement, which proves the accuracy of the mechanical analysis, thereby confirming the reinforcing effect of nanocellulose on starch-based bio-nanocomposites.

5. Conclusions

Starch-nanocellulose bio-nanocomposite films were successfully fabricated and systematically characterized to investigate the effect of nanocellulose fiber loading on their physicochemical, structural, thermal, optical, and mechanical properties. The results clearly demonstrate that incorporating nanocellulose significantly enhances the performance of starch-based films.

View Article Online
DOI: 10.1039/D6NA00060F

Because starch is naturally hygroscopic and contains glycerol, clean starch films have the highest hydrophilicity, according to tests of water uptake and moisture absorption. In contrast, increasing nanocellulose content significantly decreased both water uptake and moisture absorption. Strong hydrogen bonds between starch and nanocellulose are thought to be the cause of this decrease in free volume and limited molecular mobility inside the starch matrix. Additional solubility tests revealed that the composite films had strong chemical resistance and only dissolve in dimethyl sulphoxide, supporting their appropriateness for real-world uses. Pure starch films were brittle and broken, according to morphological studies, whereas films reinforced with nanocellulose were continuous and free of cracks, indicating better interfacial compatibility and film integrity. Morphological analysis confirmed that nanocellulose effectively improved film continuity and eliminated cracking, while solubility tests revealed good chemical resistance, with films remaining stable in most solvents except dimethyl sulfoxide. A gradual increase in crystallinity from 32% for pure starch to 60% for films containing 20 wt % nanocellulose was confirmed by XRD analysis, highlighting the function of nanocellulose as an effective nucleating and reinforcing agent. Due to increased crystallinity and light dispersion, optical experiments revealed a progressive decrease in light transmittance with increasing nanocellulose loading, while maintaining adequate transparency without obvious fiber aggregation. Larger degradation temperatures were noted at larger nanocellulose concentrations, especially at 20 weight percent, according to thermal analysis, which showed increased thermal stability of the composites. Although elongation at break reduced due to increased stiffness, mechanical testing showed considerable gains in tensile strength and Young's modulus with increasing nanocellulose loading, indicating the strong reinforcing impact of nanocellulose. All these results demonstrate that nanocellulose is a useful reinforcement for starch matrices, allowing for the creation of biodegradable and sustainable films with enhanced mechanical, thermal, structural, and physicochemical properties for packaging applications. For a more thorough assessment, more research on comprehensive barrier characteristics such gas permeability and water vapor transmission is advised.

View Article Online
DOI: 10.1039/D6NA00060F

Conflict of Interest

The authors declare that they have no known financial or personal conflicts of interest that could have influenced the work reported in this paper.

Data Availability Statement

The data supporting the findings of this study can be obtained from the corresponding author upon request. Due to privacy concerns and other restrictions, the data are not publicly accessible.

Acknowledgements

The authors extend their sincere thanks to the Dept. of Applied Chemistry & Chemical Engineering, Islamic University, Bangladesh, for providing a supportive research environment and essential facilities. The authors are also thankful to the Chemistry Discipline, Khulna University, for providing supportive research facilities.

References

1. Jambeck, J.R. and I. Walker-Franklin, *The impacts of plastics' life cycle.* One Earth, 2023. **6**(6): p. 600-606.
2. Ahmed, D.M., et al., *Advances in Bio-Based Regenerated and Synthetic Fibres and Their Sustainability Issues*, in *SDG 12 and Global Fashion Textiles Production*. 2025, Springer. p. 65-100.
3. Mukherjee, C., et al., *Recent advances in biodegradable polymers–properties, applications and future prospects.* European Polymer Journal, 2023. **192**: p. 112068.
4. Ahmed, A.S., et al., *Microalgae to Biofuel: Cutting-Edge Harvesting and Extraction Methods for Sustainable Energy Solution.* Energy Science & Engineering, 2025. **13**(7): p. 3525-3540.
5. Sunday, N.F., et al., *Iron (III) oxide and Silver oxide-Chromolaena odorata leaf biochar nanocomposites as effective bio-inorganic material for the treatment of borehole water.* Discover Hazards, 2026. **2**(1): p. 14.
6. Sharma, D., et al., *Thermal Techniques for the Degradation and Remediation of Microplastics*, in *Microplastics*. 2025, CRC Press. p. 66-85.

7. Correa Pinto, B., et al., *Arrowroot Starch/ZnO Nanoparticle Nanocomposite Films: Thermal, Morphological, and Tensile Properties.* ACS omega, 2025. **10**(27): p. 28920-28931.
8. Santos, M.B., et al., *Corn starch/Carboxymethyl Cellulose Films: Influence of Citric Acid on Water Susceptibility, Morphological and Tensile Properties.* ACS Omega, 2026.
9. de Souza, R.F. and M.A. Spinacé, *Biocomposites of thermoplastic starch/viscose waste: Processing and characterization.* Next Materials, 2026. **10**: p. 101423.
10. Khouaja, A., A. Koubaa, and H.B. Daly, *Mechanical and morphological properties of cellulose biocomposites.* Chemosphere, 2025. **379**: p. 144415.
11. Kunnath, S.M., et al., *Nanocellulose-Based Composites as Advanced Materials.* 2024.
12. Kumar, A., et al., *Nanocellulose: A Comprehensive Review of Sustainable Applications and Innovations.* Journal of Renewable Materials, 2025. **13**(7).
13. Ren, H., et al., *Preparation and characterization of starch-based composite films reinforced by quinoa (Chenopodium quinoa Willd.) straw cellulose nanocrystals.* International Journal of Biological Macromolecules, 2023. **242**: p. 124938.
14. Ghamari, M., et al., *Nanocellulose extraction from biomass waste: unlocking sustainable pathways for biomedical applications.* The Chemical Record, 2025. **25**(5): p. e202400249.
15. Joshi, G., S. Shukla, and S.S. Chauhan, *Nanocellulose extraction from lignocellulosic materials and its potential applications: a review.* Journal of the Indian Academy of Wood Science, 2024. **21**(1): p. 1-23.
16. Koshy, J.T. and D. Sangeetha, *Nanocellulose reinforced sustainable polyvinyl alcohol and pectin based nanocomposite films embedded with AgO/ZnO nano structures for wound dressing applications.* Scientific Reports, 2026.
17. Wodag, A.F. and A. Azanaw, *A review of nanocellulose composite materials: Manufacturing, properties, applications, current challenges and future outlooks.* Carbohydrate Polymer Technologies and Applications, 2026: p. 101093.
18. Mahardika, M., et al., *Revolutionizing thermoplastic starch: Advances in nanocellulose reinforced biocomposites: A review.* Biomass and Bioenergy, 2026. **204**: p. 108419.
19. Zhao, X., et al., *Environment Friendly, Renewable and Sustainable Natural Fiber-Reinforced Polylactic Acid (PLA) Composites.* Polymer Composites, 2026.

20. Kakehbaraei, S., M. Arab-Zozani, and S. Kakebaraei, *Emerging trends in viral infection inhibition using a chitosan-based drug delivery system.* Journal of Drug Targeting, 2026. **34**(1): p. 41-56.
21. Hu, C., et al., *Multimodal SERS biosensing platforms: Emerging opportunities for ultrasensitive biomarker detection and intelligent diagnostics.* ACS sensors, 2026. **40**(XXX): p. XXX-XXX.
22. Tahir, D., et al., *Sources, chemical functionalization, and commercial applications of nanocellulose and nanocellulose-based composites: a review.* Polymers, 2022. **14**(21): p. 4468.
23. Balakrishnan, P., et al., *UV resistant transparent bionanocomposite films based on potato starch/cellulose for sustainable packaging.* Starch-Stärke, 2018. **70**(1-2): p. 1700139.
24. Tabatabaei, M.R., et al., *Poly (butylene succinate) Based Biocomposites Incorporating Thermoplastic Millet Starch and Microcrystalline Cellulose.* Carbohydrate Polymer Technologies and Applications, 2026: p. 101112.
25. Karavasili, D., et al., *Biobased Polymers in Printed Electronics: From Renewable Resources to Functional Devices.* Polymers, 2026. **18**(2): p. 301.
26. Beer, F.P., et al., *Mechanics of materials*. 2006, McGraw Hill.
27. Balakrishnan, P., et al., *Morphology, transport characteristics and viscoelastic polymer chain confinement in nanocomposites based on thermoplastic potato starch and cellulose nanofibers from pineapple leaf.* Carbohydrate polymers, 2017. **169**: p. 176-188.
28. Biswas, S.K., et al., *Bionanofiber-reinforced transparent nanocomposites for future applications*, in *Applications of Multifunctional Nanomaterials*. 2023, Elsevier. p. 297-325.
29. Medina-Jaramillo, C., et al., *Starch-based biocomposites reinforced with cellulose nanofibers from potato peel byproducts.* Scientific Reports, 2025. **15**(1): p. 38412.

View Article Online
DOI: 10.1039/D6NA00060F

Data Availability Statement: The data supporting the findings of this study can be obtained from the corresponding author upon request. Due to privacy concerns and other restrictions, the data are not publicly accessible.